Nuclear Science and Techniques (2024) 35:180
https://doi.org/10.1007/s41365-024-01557-4

Investigation of multinucleon transfer processes in the Langevin equation model

Ying Zou[1,2] · Ming-Hao Zhang[1,2] · Mei-Chen Wang[1,2] · Yu-Hai Zhang[1,2] · Feng-Shou Zhang[1,2,3]

Received: 31 May 2024 / Revised: 14 July 2024 / Accepted: 18 July 2024 / Published online: 27 September 2024

Abstract
Multinucleon transfer in low-energy heavy-ion collisions is increasingly considered a promising approach for generating exotic nuclei. Understanding the complex mechanisms involved in multinucleon transfer processes presents significant challenges for the theoretical investigation of nuclear reactions. A Langevin equation model was developed and employed to investigate multinucleon transfer processes. The ^{40}Ar + ^{232}Th reaction was simulated, and the calculated Wilczyński plot was used to verify the model. Additionally, to study the dynamics of multinucleon transfer reactions, the ^{136}Xe + ^{238}U and ^{136}Xe + ^{209}Bi reactions were simulated, and the corresponding TKE-mass and angular distributions were computed to analyze the energy dissipation and scattering angles. This investigation enhances our understanding of the dynamics involved in multinucleon transfer processes.

Keywords Reaction mechanisms · Multinucleon transfer reactions · Langevin equations · Wilczyński plot · Exotic nuclei

1 Introduction

Between 1969 and 1995, approximately 75 new neutron-rich nuclides were discovered via multinucleon transfer (MNT) reactions [1]; however, no new transuranium or superheavy nuclides were detected using MNT reactions. The constraints of projectile fragmentation (PF) and fusion-evaporation (FE) reactions have rekindled interest in MNT for generating exotic nuclei, particularly those in the N=126 and superheavy regions [2–5].

Zagrebaev et al. first proposed that the reaction ^{136}Xe +^{208} Pb at energies near the Coulomb barrier was suitable for creating new neutron-rich isotopes near the neutron shell closure at N = 126 [6]. More than 50 unknown nuclei may be produced in such a reaction with cross sections of not less than 1μb. Building on this, Dubna conducted MNT reaction experiments in 2012 with ^{136}Xe +^{208} Pb [7], which resulted in the transfers of up to 16 nucleons from Xe to Pb. Experimental results from the ^{136}Xe +^{198} Pt reaction obtained at Grand Accélérateur National d'Ions Lourds (GANIL) in 2015 revealed that the cross sections for producing N = 126 nuclei in MNT reactions significantly exceed those from PF [8]. Most recently, Dubna reported the transfer of approximately 27 nucleons from the projectile to the target nucleus in the ^{136}Xe +^{238} U reaction [9]. MNT reactions can also be used to synthesize transuranium nuclei. In 2018, experiments conducted at Texas A &M University using the ^{238}U +^{232} Th reaction compared the energies and half-lives of alpha emitters with known and predicted values, revealing the production of new elements with atomic numbers up to 116 [10]. A breakthrough in the production of new nuclides using the MNT process was the reaction ^{48}Ca +^{248} Cm conducted at GSI [11]. Five new neutron-deficient isotopes, including ^{216}U, ^{219}Np, ^{223}Am, ^{229}Am and ^{233}Bk were discovered. In 2023, Niwase et al. synthesized the new neutron-rich isotope ^{241}U via the

This work was supported by the National Key R &D Program of China (No. 2023YFA1606401) and the National Natural Science Foundation of China (Nos. 12135004, 11635003 and 11961141004).

✉ Feng-Shou Zhang
fszhang@bnu.edu.cn

[1] The Key Laboratory of Beam Technology of Ministry of Education, School of Physics and Astronomy, Beijing Normal University, Beijing 100875, China

[2] Institute of Radiation Technology, Beijing Academy of Science and Technology, Beijing 100875, China

[3] Center of Theoretical Nuclear Physics, National Laboratory of Heavy Ion Accelerator of Lanzhou, Lanzhou 730000, China

MNT reaction ^{238}U +^{198} Pt at the KEK Isotope Separation System (KISS) facility [12].

The MNT reactions involve quasi-elastic (QE), deep inelastic (DI), and quasi-fission (QF) processes. The ^{40}Ar + ^{232}Th reaction is a representative experiment illustrating the dynamic mechanism of the MNT reactions[13]. Subsequently, Wilczyński effectively explained this experiment based on friction theory and scattering into negative angles [14].

The theoretical frameworks employed in investigating the MNT reactions include both phenomenological and microscopic models. Phenomenological approaches include the Langevin equations [15–22], GRAZING model [23–25], and dinuclear system (DNS) model [26–43]. Microscopic approaches include the improved quantum molecular dynamics model (ImQMD) [44–50] and time-dependent Hartree-Fock approach (TDHF) [51–55]. These theoretical models of heavy-ion collisions have guided the production of new exotic nuclei [56–64].

To comprehensively analyze heavy-ion collisions, Zagrebaev and Greiner applied the Langevin equations to MNT reactions, covering the entire process from the entrance stage to the formation of the fused system, including the DI, QF, and fission processes. They used the evolution of mass asymmetry to describe nucleon transfer [16, 17] and subsequently introduced charge asymmetry as a degree of freedom to account for the equilibration of the neutron-to-proton ratio [18, 19]. Subsequent studies further developed the Langevin model [65–68]. As a phenomenological framework, the current Langevin approach considers only microscopic effects by incorporating the shell correction energy into the driving potential, regardless of other phenomena. Therefore, to improve the Langevin approach for self-consistently simulating MNT processes including microscopic mechanisms, a Langevin equation model was developed by simplifying the current framework and was employed to simulate the dynamics of MNT reactions in the initial stage. Calculations of the Wilczyński plot were used to verify that the simplified model adequately described energy dissipation and angular distributions, thereby demonstrating that fluctuation-dissipation in the friction mechanism primarily affects energy dissipation during MNT reactions, particularly for the DI and QF processes.

The remainder of this article is organized as follows: Sect. 2 introduces the Langevin equations, while Sect. 3 presents the results and discussion. Finally, a summary of this work is presented in Sect. 4.

2 Theoretical model

In this study, we employed a two-center parameterization to describe the shape of the nuclear system [69], as shown in Fig. 1. We used three collective coordinates as follows: $z_0/R_{\rm cn}$, where z_0 is the distance between the centers of two oscillator potentials, made dimensionless by the radius of the spherical compound nucleus $R_{\rm cn}$; δ, representing the deformation of the fragment; and η_A, the mass asymmetry of the colliding nuclei, defined as $\eta_A = (A_1 - A_2)/(A_1 + A_2)$. A_1 and A_2 represent the mass numbers of the target and projectile, respectively, corresponding to the left and right components of the system. We assumed that each fragment underwent identical deformation, denoted by $\delta = \delta_1 = \delta_2$, defined by $\delta_i = (3\beta_i - 3)/(1 + 2\beta_i)$ with $\beta_i = a_i/b_i$. Here, a and b represent the half-lengths of the axes of the ellipse in the z_0 -direction and orthogonal to z_0, respectively.

The collective coordinates $q_i = \{r\ (i.e., z_0/R_{\rm cn}), \eta_{\rm A}, \delta\}$ and their conjugate momenta p_i are driven by the general form of the Langevin equations:

$$\begin{aligned}\frac{{\rm d}q_i}{{\rm d}t} &= (m^{-1})_{ij}p_j,\\ \frac{{\rm d}p_i}{{\rm d}t} &= -\frac{\partial V}{\partial q_i} - \frac{1}{2}p_j\frac{\partial (m^{-1})_{jk}}{\partial q_i}p_k - \gamma_{ij}(m^{-1})_{jk}p_k + g_{ij}\Gamma_j(t),\end{aligned} \tag{1}$$

where the shape-dependent transport coefficients m_{ij} and γ_{ij} correspond to the inertia and friction tensors, respectively. $\Gamma_i(t)$ are normalized random variables with a Gaussian distribution, and g_{ij} are the random force amplitudes determined from the fluctuation dissipation theorem, $g_{ij}g_{jk} = \gamma_{ik}T$. The nuclear temperature T is defined as $T = \sqrt{E^*/a}$, where a, the level density parameter, is assigned a constant value of $A_{\rm cn}/10$ MeV^{-1}. The excitation energy E^* is given by $E^* = E_{\rm tot} - V - E_{\rm kin}$, where the total, potential, and kinetic energies are represented by $E_{\rm tot}$ ($E_{\rm c.m.}$), V, and $E_{\rm kin} = p_j(m^{-1})_{jk}p_k/2$, respectively.

The inertia tensor components m_{ij} associated with the collective coordinates are calculated using the Werner-Wheeler approach for incompressible irrotational flow [70, 71]. Using the wall-plus-window approach of one-body dissipation, the friction tensor γ_{ij} describes the dissipation of necked-in nuclear shapes featuring two fragments connected by a well-pronounced neck [71–74]. The potential energy V includes both the rotational energy $V_{\rm rot}$ and

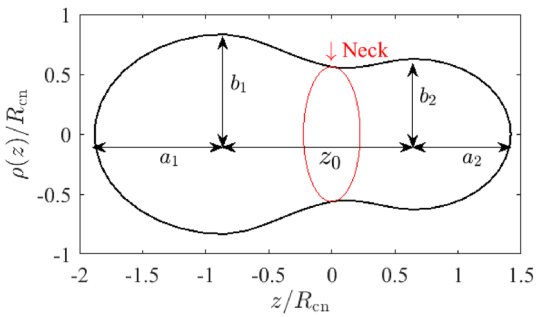

Fig. 1 The profile function $\rho(z)$ of two-center parameterization

potential energy V_{FRLDM} obtained within the finite-range liquid-drop model (FRLDM) replacing the surface energy of the liquid-drop model with a Yukawa-plus-exponential potential nuclear energy [75–78]. The formulae and parameters in our model are consistent with Eqs. (29–34) in Ref. [78]. Consequently, the potential energy utilized is adiabatic and provides the nuclear mass for a uniform charge distribution ($\eta_Z = \eta_A$).

The evolution of the angle θ, which indicates the relative orientation of the nuclei, and the relative angular momentum ℓ are governed by the following equations:

$$\begin{aligned}\frac{\mathrm{d}\theta}{\mathrm{d}t} &= \frac{\ell}{\mathfrak{I}_{12}},\\ \frac{\mathrm{d}\ell}{\mathrm{d}t} &= -\frac{\partial V}{\partial\theta} - \gamma_{\tan}\frac{\ell}{\mathfrak{I}_{12}}R^2_{\mathrm{c.m.}} + R_{\mathrm{c.m.}}\sqrt{\gamma_{\tan}T}\,\Gamma_{\tan}(t).\end{aligned} \tag{2}$$

Here, $\mathfrak{I}_{12}$ is the inertia moment of the relative motion; $R_{\mathrm{c.m.}}$ is the distance between the mass centers of the nuclei; and $\gamma_{\tan}$ is the tangential friction force of the colliding nuclei. $\gamma_{\tan}$ is assumed to vary with the radial friction $\gamma_{\tan} = \gamma^0_{\tan}\gamma_{\mathrm{rr}}$, where $\gamma^0_{\tan}$ is an adjustable parameter.

Two-center parameterization employs ϵ to describe the neck of a mononucleus system. To reduce the computational complexity, we assume that ϵ evolves over time instead of being included as a collective coordinate. The value of ϵ shifts from 1 in the entrance channel to 0.35 in the exit channel [79]. Therefore, the potential energy also undergoes a transition from entrance to exit as follows:

$$\begin{aligned}V(q;\tau) &= V(q,\epsilon=1)f_\epsilon(\tau) + V(q,\epsilon=0.35)[1-f_\epsilon(\tau)],\\ f(\tau) &= \exp\left(-\tau/\tau_\epsilon\right),\end{aligned} \tag{3}$$

where τ represents the relaxation time of the neck and τ_ϵ is the parameter whose suggested value is 10^{-21} s [20].

Notably, if nucleon transfer is considered under the evolution of mass asymmetry η_A driven by Eq. (1), the friction γ_r and γ_{η_A} are zero before the two separated nuclei come into contact and form mononucleus, indicating the absence of nucleon transfer. However, this does not correspond to reality, particularly when simulating large-impact parameters and grazing processes, where it diverges from experimental results. Consequently, to describe nucleon transfer before the contact point, this study employs the inertialess-reduced Langevin equation [16], which is derived from the corresponding master equation for the distribution function [80]. Because of the different equations used to calculate nucleon transfer at various stages, their transition requires further consideration.

Initially, Zagrebaev and Greiner utilized inertialess-reduced Langevin equations for mass and charge asymmetries to comprehensively handle the nucleon transfer process without considering the momentum and kinetic energy of mass asymmetry [16–18]. Karpov and Saiko further developed the model by solving the full Langevin equations, which also incorporated mass and charge fluctuations [20–22]. Referring to these studies, the approach employed in this study employs two different equations for the separated and mononucleus stages. In addition, our model is simplified from the aforementioned studies as follows: In selecting the collective coordinates, identical deformations were assumed for both nuclei; the intrinsic rotation of the nuclei was neglected; the potential energy was described using the FRLDM, without considering shell correction energy and the initial sudden approximation; and the use of phenomenological friction in the entrance channel was eliminated to reduce the number of model parameters.

3 Results and discussion

3.1 Wilczyński plot for ^{40}Ar + ^{232}Th system

Trajectory calculations start at $r = 5$, which for the ^{40}Ar + ^{232}Th system is equivalent to a distance of 40 fm between the centers of mass of the projectile and target nuclei. In addition, the excitation energies of the initial conditions were set to zero. At the scission point, the nuclei were separated, resulting in the formation of primary fragments, which marked the termination of the calculation. Five hundred events were simulated for each impact parameter.

Wilczyński proposed constructing a contour map of the double differential cross section on the energy and scattering angle plane [14], known as the Wilczyński plot for studying the dynamics of nucleus–nucleus collisions. This allows the analysis of the relationship between the dissipation of total kinetic energy (TKE) and rotational degrees of freedom from the various quantities involved in the MNT reaction. We calculated the Wilczyński plot for ^{40}Ar + ^{232}Th system shown in Fig. 2 at $E_{\mathrm{lab}} = 388$ MeV ($E_{\mathrm{c.m.}} = 331$ MeV).

Although the friction model has effectively conformed to the peaks observed in the Wilczyński plot [81], it fails to describe the statistical fluctuations. Peaks resembling those predicted by the friction model are obtained when the fluctuation component is turned off. By comparing this curve with the experimental data, we can adjust the model parameters $\gamma_{\tan}$, τ_ϵ. In the simulation, the energy dissipation and angular evolution of the DI and QF processes were consistent with the experimental results. In addition, we observed trajectories with negative deflection angles. For instance, Fig. 3 shows one such trajectory for angular momentum $L = 100\hbar$ with a deflection angle of $\theta_{\mathrm{c.m.}} = -27°$.

Because $\gamma^0_{\tan}$ is a model parameter that determines the rate of angular momentum dissipation, it can manifest in the relationship between the calculated TKE and scattering angle. Therefore, prior to simulation, $\gamma^0_{\tan}$ must be adjusted based on the peak of experimental Wilczyński plot. The value of

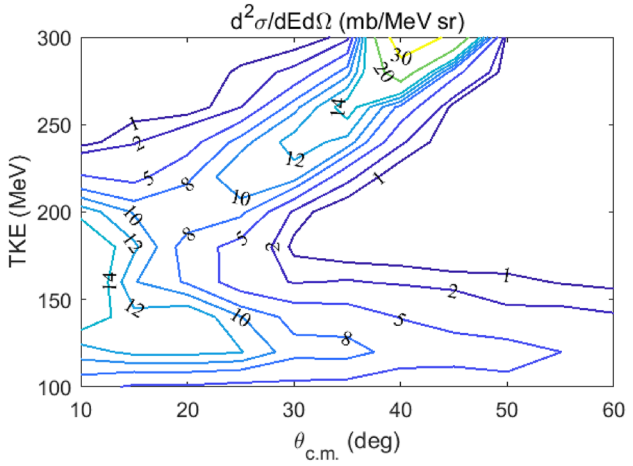

Fig. 2 (Color online) Calculated Wilczyński plot for the ^{40}Ar + ^{232}Th collision at E_{lab} = 388 MeV

γ^0_{tan} is set to 0.05 in Fig. 2. However, experimental data for the Wilczyński plot are unavailable for all systems. For such systems, the adjustment of γ^0_{tan} can be guided by the Sommerfeld-like parameter $\eta' = \frac{Z_1 Z_2 \sqrt{\mu}}{\hbar\sqrt{2(E_{c.m.} - V_B)}}$ [82], where μ and V_B are the reduced mass and Coulomb barrier, respectively. For systems with η' less than 200, such as the ^{40}Ar + ^{232}Th reaction with η' = 120, the peak of the Wilczyński plot shifted toward negative angles as the total kinetic energy loss (TKEL) increased. However, when η' increased to 400, the peak tended to stabilize in the direction of the constant scattering angle. The peak progressively extended toward larger scattering angles with further increase in η'.

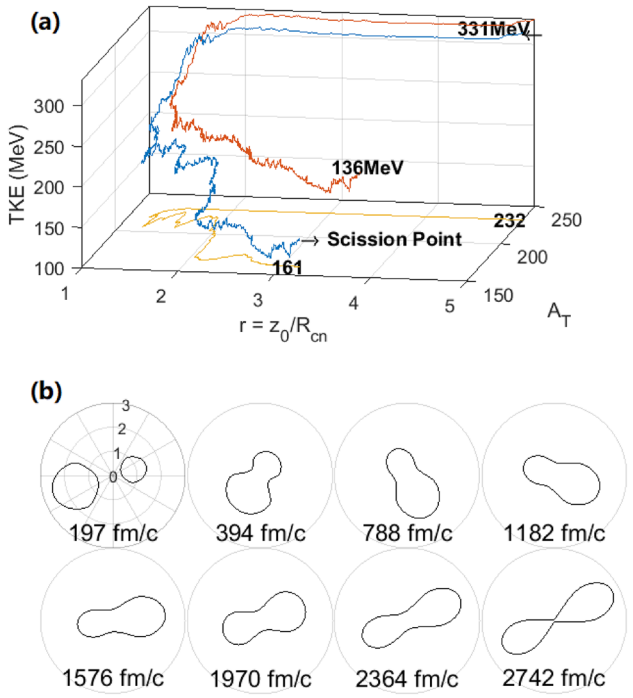

Fig. 3 (Color online) Trajectory for the ^{40}Ar + ^{232}Th collision at E_{lab} = 388 MeV: **a** Trajectory and its projections of the evolution of energy ($V + E_{kin}$), elongation, and mass of heavier nucleus; **b** Profile of the trajectory at the indicated time

3.2 Calculations for ^{136}Xe + ^{238}U, ^{209}Bi systems

For further comparison with the experimental data, we simulated the ^{136}Xe + ^{238}U reaction at E_{lab} = 1110 MeV ($E_{c.m.}$ = 706.4 MeV). The average TKE and total excitation energy E^*_{total} for the fragments, calculated as a function of the primary fragment mass, are presented in Fig. 4, along with a comparison with experimental results [9].

The calculated energy dissipation for large mass transfers is consistent with the experimental results, indicating that the simulation of the average TKE for fragment masses below 230 is reasonable. However, Langevin calculations for target-like fragments (TLFs) significantly underestimate the dissipated energy in the reaction, particularly in cases involving fewer nucleon transfers because of the simplified descriptions near the contact point. The results (Fig. 4) include only trajectories where the two nuclei come into contact. Trajectories involving grazing processes, in which the two nuclei did not directly touch under large collision parameters, were excluded.

We simulated the ^{136}Xe + ^{209}Bi reaction for E_{lab} = 1130 MeV ($E_{c.m.}$ = 684 MeV). In Fig. 5, the center-of-mass angular distribution $d\sigma/d\Omega$ of the differential cross section is plotted versus $\theta_{c.m.}$ for events corresponding to TKE between 300 and 650 MeV. The angular distribution is consistent with the experimental values, except for the region near

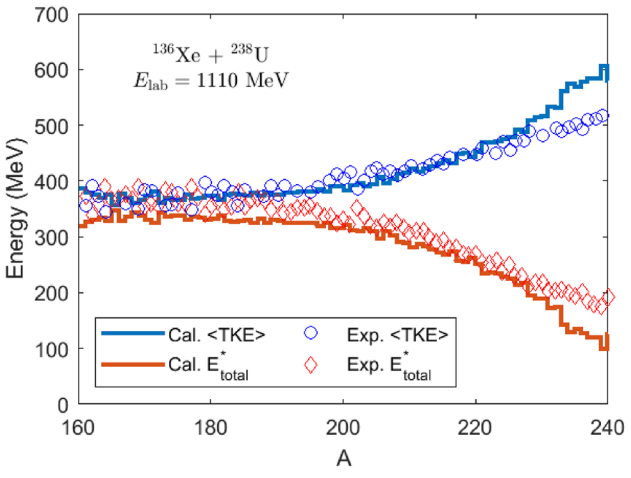

Fig. 4 (Color online) Average TKE and E^*_{total} calculated as a function of the primary fragment mass. The empty symbols correspond to the experimental results [9]

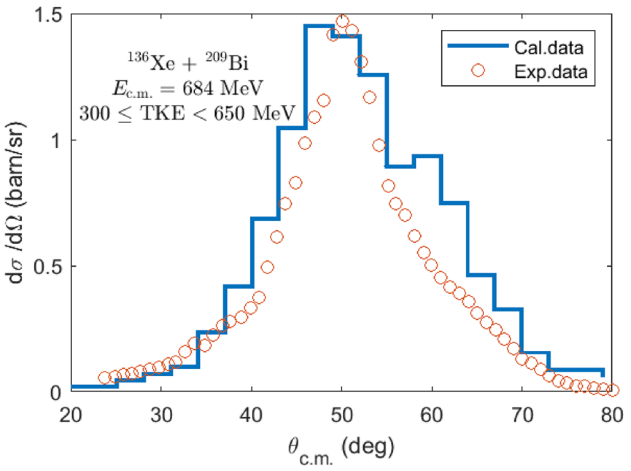

Fig. 5 (Color online) Center-of-mass angular distribution of the damped cross section for events with TKE within the indicated range in the ^{136}Xe + ^{209}Bi reaction at E_{lab} = 1130 MeV. The experimental data are from [83]. Histogram is the calculation

$\theta_{gr} + 10°$. The grazing angle θ_{gr} for this reaction is 54°. This discrepancy can also be attributed to the description of the model before the contact point. In particular, for heavy systems, the continuous use of FRLDM as the potential energy is unsuitable for the approach stage. Therefore, the model requires further refinement to describe the separated stage. γ^0_{tan} was set to 0.11 for the ^{136}Xe + ^{238}U and ^{136}Xe + ^{209}Bi reactions.

The interaction time, τ_{int}, is a fundamental characteristic of nuclear reactions, which represents the time from when the two nuclei contact each other until they subsequently separate into fragments, as illustrated in Fig. 6 for the studied reactions. In addition, the distributions of the total simulation time t_{tot}, starting from $t = 0$ at $r = 5$, are presented. These include trajectories with grazing collisions under large impact parameters. Longer interaction times within these distributions correspond to the most dissipative collisions, such as the QF process.

4 Summary

In this study, a Langevin equation model was developed to simplify previous research by reducing the number of adjustable model parameters and streamlining the physical processes considered. This model was employed to investigate multinucleon transfer processes, enabling the analysis of double differential cross sections across energy and scattering angles. The classical ^{40}Ar + ^{232}Th reaction was simulated at E_{lab} = 388 MeV, and the calculated Wilczyński plot was displayed. For comparisons with experimental results, the ^{136}Xe + ^{238}U reaction was simulated at E_{lab} = 1110 MeV, alongside the ^{136}Xe + ^{209}Bi

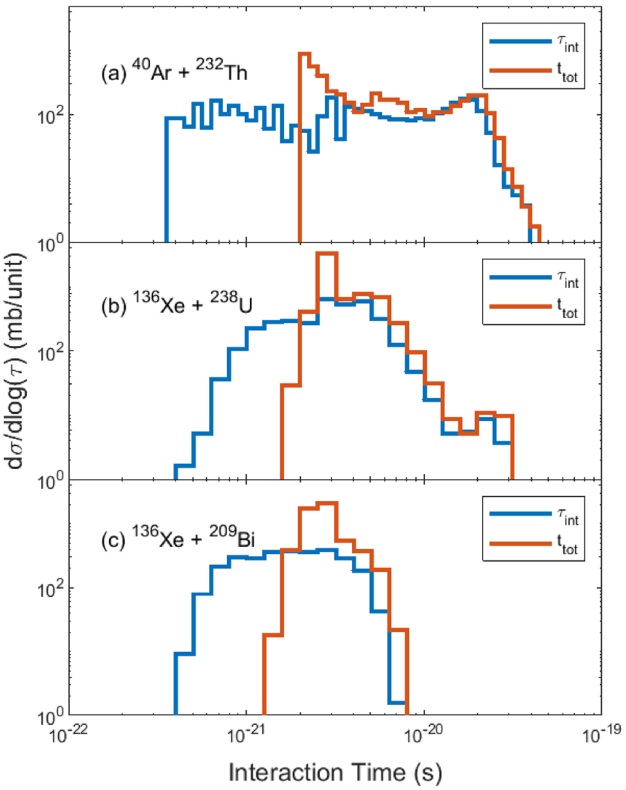

Fig. 6 (Color online) Reaction time distributions for the **a** ^{40}Ar + ^{232}Th collision at E_{lab} = 388 MeV, **b** ^{136}Xe + ^{238}U reaction at E_{lab} = 1.11 GeV, and **c** ^{136}Xe + ^{209}Bi reaction at E_{lab} = 1130 MeV

reaction at E_{lab} = 1130 MeV, with subsequent calculations of TKE-mass distributions and angular distributions, respectively. Finally, the interaction time distributions of the reactions were calculated. These results indicate that the simplified Langevin equation model effectively describes the energy dissipation in MNT reactions.

Author contributions All authors contributed to the study conception and design. Material preparation, data collection and analysis were performed by Ying Zou, Mei-Chen Wang and Ming-Hao Zhang. The first draft of the manuscript was written by Ying Zou, and all authors commented on previous versions of the manuscript. All authors read and approved the final manuscript.

Data availability The data that support the findings of this study are openly available in Science Data Bank at https://cstr.cn/31253.11.sciencedb.j00186.00256 and https://doi.org/10.57760/sciencedb.j00186.00256.

Declarations

Conflict of interest Feng-Shou Zhang is an editorial board member for Nuclear Science and Techniques and was not involved in the editorial review, or the decision to publish this article. All authors declare that there are no Conflict of interest.

References

1. G.G. Adamian, N.V. Antonenko, A. Diaz-Torres et al., How to extend the chart of nuclides? Eur. Phys. J. A **56**(2), 47 (2020). https://doi.org/10.1140/epja/s10050-020-00046-7
2. F.-S. Zhang, C. Li, L. Zhu et al., Production cross sections for exotic nuclei with multinucleon transfer reactions. Front. Phys. **13**(6), 132113 (2018). https://doi.org/10.1007/s11467-018-0843-6
3. R. Ogul, N. Buyukcizmeci, A. Ergun et al., Production of neutron-rich exotic nuclei in projectile fragmentation at Fermi energies. Nucl. Sci. Tech. **28**, 18 (2016). https://doi.org/10.1007/s41365-016-0175-6
4. F.-S. Zhang, Y.-H. Zhang, M.-H. Zhang et al., Synthesis of new superheavy nuclei. J. Beijing Nor. Univ. **58**, 392–399 (2022). https://doi.org/10.12202/j.0476-0301.2022082
5. Y.-H. Zhang, G. Zhang, J.-J. Li et al., Progress in the production of new radioactive nuclides based on large-scale scientific facilities. J. Isotopes **35**(2), 104–113 (2022). https://doi.org/10.7538/tws.2022.35.02.0104
6. V. Zagrebaev, W. Greiner, Production of new heavy isotopes in low-energy multinucleon transfer reactions. Phys. Rev. Lett. **101**, 122701 (2008). https://doi.org/10.1103/PhysRevLett.101.122701
7. E.M. Kozulin, E. Vardaci, G.N. Knyazheva et al., Mass distributions of the system 136 Xe + 208 Pb at laboratory energies around the Coulomb barrier: a candidate reaction for the production of neutron-rich nuclei at N = 126. Phys. Rev. C **86**, 044611 (2012). https://doi.org/10.1103/PhysRevC.86.044611
8. Y.X. Watanabe, Y.H. Kim, S.C. Jeong et al., Pathway for the production of neutron-rich isotopes around the $N = 126$ shell closure. Phys. Rev. Lett. **115**, 172503 (2015). https://doi.org/10.1103/PhysRevLett.115.172503
9. E.M. Kozulin, G.N. Knyazheva, A.V. Karpov et al., Detailed study of multinucleon transfer features in the ^{136}Xe +^{238} U reaction. Phys. Rev. C **109**, 034616 (2024). https://doi.org/10.1103/PhysRevC.109.034616
10. S. Wuenschel, K. Hagel, M. Barbui et al., Experimental survey of the production of α-decaying heavy elements in ^{238}U +^{232} Th reactions at 7.5–6.1 MeV/nucleon. Phys. Rev. C **97**, 064602 (2018). https://doi.org/10.1103/PhysRevC.97.064602
11. H. Devaraja, S. Heinz, O. Beliuskina et al., Observation of new neutron-deficient isotopes with $Z \geq 92$ in multinucleon transfer reactions. Phys. Lett. B **748**, 199–203 (2015). https://doi.org/10.1016/j.physletb.2015.07.006
12. T. Niwase, Y.X. Watanabe, Y. Hirayama et al., Discovery of new isotope ^{241}U and systematic high-precision atomic mass measurements of neutron-rich pa-pu nuclei produced via multinucleon transfer reactions. Phys. Rev. Lett. **130**, 132502 (2023). https://doi.org/10.1103/PhysRevLett.130.132502
13. A. Artukh, G. Gridnev, V. Mikheev et al., Transfer reactions in the interaction of ^{40}Ar with ^{232}Th. Nucl. Phys. A **215**, 91–108 (1973). https://doi.org/10.1016/0375-9474(73)90104-8
14. J. Wilczyński, Nuclear molecules and nuclear friction. Phys. Lett. B **47**, 484–486 (1973). https://doi.org/10.1016/0370-2693(73)90021-X
15. P. Fröbrich, I.I. Gontchar, Langevin description of fusion, deep-inelastic collisions and heavy-ion-induced fission. Phys. Rep. **292**, 131–237 (1998). https://doi.org/10.1016/S0370-1573(97)00042-2
16. V. Zagrebaev, W. Greiner, Unified consideration of deep inelastic, quasi-fission and fusion-fission phenomena. J. Phys. G Nucl. Part. Phys. **31**, 825–844 (2005). https://doi.org/10.1088/0954-3899/31/7/024
17. V. Zagrebaev, W. Greiner, Low-energy collisions of heavy nuclei: dynamics of sticking, mass transfer and fusion. J. Phys. G Nucl. Part. Phys. **34**, 1–25 (2007). https://doi.org/10.1088/0954-3899/34/1/001
18. V.I. Zagrebaev, W. Greiner, Production of heavy and superheavy neutron-rich nuclei in transfer reactions. Phys. Rev. C **83**, 044618 (2011). https://doi.org/10.1103/PhysRevC.83.044618
19. V. Zagrebaev, W. Greiner, Cross sections for the production of superheavy nuclei. Nucl. Phys. A **944**, 257–307 (2015). https://doi.org/10.1016/j.nuclphysa.2015.02.010
20. A.V. Karpov, V.V. Saiko, Modeling near-barrier collisions of heavy ions based on a Langevin-type approach. Phys. Rev. C **96**, 024618 (2017). https://doi.org/10.1103/PhysRevC.96.024618
21. V.V. Saiko, A.V. Karpov, Analysis of multinucleon transfer reactions with spherical and statically deformed nuclei using a Langevin-type approach. Phys. Rev. C **99**, 014613 (2019). https://doi.org/10.1103/PhysRevC.99.014613
22. V. Saiko, A. Karpov, Multinucleon transfer as a method for production of new heavy neutron-enriched isotopes of transuranium elements. Eur. Phys. J. A **58**, 41 (2022). https://doi.org/10.1140/epja/s10050-022-00688-9
23. A. Winther, Grazing reactions in collisions between heavy nuclei. Nucl. Phys. A **572**, 191–235 (1994). https://doi.org/10.1016/0375-9474(94)90430-8
24. A. Winther, Dissipation, polarization and fluctuation in grazing heavy-ion collisions and the boundary to the chaotic regime. Nucl. Phys. A **594**, 203–245 (1995). https://doi.org/10.1016/0375-9474(95)00374-A
25. R. Yanez, W. Loveland, Predicting the production of neutron-rich heavy nuclei in multinucleon transfer reactions using a semi-classical model including evaporation and fission competition. Grazing-F. Phys. Rev. C **91**(4), 04460 (2015). https://doi.org/10.1103/PhysRevC.91.044608
26. V.V. Volkov, Deep inelastic transfer reactions - the new type of reactions between complex nuclei. Phys. Rep. **44**, 93–157 (1978). https://doi.org/10.1016/0370-1573(78)90200-4
27. G.G. Adamian, N.V. Antonenko, W. Scheid et al., Treatment of competition between complete fusion and quasifission in collisions of heavy nuclei. Nucl. Phys. A **627**, 361–378 (1997). https://doi.org/10.1016/S0375-9474(97)00605-2
28. G.G. Adamian, N.V. Antonenko, D. Lacroix, Production of neutron-rich Ca, Sn, and Xe isotopes in transfer-type reactions with radioactive beams. Phys. Rev. C **82**, 064611 (2010). https://doi.org/10.1103/PhysRevC.82.064611
29. Z.-Q. Feng, Production of neutron-rich isotopes around $N = 126$ in multinucleon transfer reactions. Phys. Rev. C **95**(2), 024615 (2017). https://doi.org/10.1103/PhysRevC.95.024615
30. C. Li, P.-W. Wen, J.-J. Li et al., Production of heavy neutron-rich nuclei with radioactive beams in multinucleon transfer reactions. Nucl. Sci. Tech. **28**, 110 (2017). https://doi.org/10.1007/s41365-017-0266-z
31. L. Zhu, J. Su, W.-J. Xie et al., Theoretical study on production of heavy neutron-rich isotopes around the $N = 126$ shell closure in radioactive beam induced transfer reactions. Phys. Lett. B **767**, 437–442 (2017). https://doi.org/10.1016/j.physletb.2017.01.082
32. M.-H. Mun, K. Kwak, G.G. Adamian et al., Possible production of neutron-rich no isotopes. Phys. Rev. C **101**, 044602 (2020). https://doi.org/10.1103/PhysRevC.101.044602
33. G. Zhang, J.-J. Li, X.-R. Zhang et al., Role of the quasifission yields in the multinucleon transfer reactions of ^{136}Xe +^{208} Pb. Phys. Rev. C **102**, 024617 (2020). https://doi.org/10.1103/PhysRevC.102.024617
34. F. Niu, P.-H. Chen, H.-G. Cheng, Z.-Q. Feng, Multinucleon transfer dynamics in nearly symmetric nuclear reactions. Nucl. Sci. Tech. **31**, 59 (2020). https://doi.org/10.1007/s41365-020-00770-1
35. J.-J. Li, N. Tang, Y.-H. Zhang et al., Theoretical study on the production of neutron-rich transuranium nuclei with radioactive beams in multinucleon transfer reactions. Phys. Rev. C **106**, 014606 (2022). https://doi.org/10.1103/PhysRevC.106.014606

36. L. Zhu, J. Su, C. Li et al., How to approach the island of stability: reactions using multinucleon transfer or radioactive neutron-rich beams? Phys. Lett. B **829**, 137113 (2022). https://doi.org/10.1016/j.physletb.2022.137113
37. X.-J. Bao, S.-Q. Guo, P.H. Chen, Production of new neutron-rich isotopes with $92 \leq Z \leq 100$ in multinucleon transfer reactions. Phys. Rev. C **105**, 024610 (2022). https://doi.org/10.1103/PhysRevC.105.024610
38. N. Tang, X.-R. Zhang, J.-J. Li et al., Production of unknown neutron-rich isotopes with $Z = 99 - 102$ in multinucleon transfer reactions near the Coulomb barrier. Phys. Rev. C **106**, 034601 (2022). https://doi.org/10.1103/PhysRevC.106.034601
39. Y.-H. Zhang, J.-J. Li, N. Tang et al., Production cross sections of new neutron-rich isotopes with $Z = 92 - 106$ in the multinucleon transfer reaction ^{197}Au $+^{232}$ Th. Phys. Rev. C **107**, 024604 (2023). https://doi.org/10.1103/PhysRevC.107.024604
40. Z. Liao, L. Zhu, J. Su et al., Dynamics of charge equilibration and effects on producing neutron-rich isotopes around $N = 126$ in multinucleon transfer reactions. Phys. Rev. C **107**, 014614 (2023). https://doi.org/10.1103/PhysRevC.107.014614
41. P.-H. Chen, C. Geng, Z.-X. Yang et al., Production of neutron-rich actinide isotopes in isobaric collisions via multinucleon transfer reactions. Nucl. Sci. Tech. **34**(10), 160 (2023). https://doi.org/10.1007/s41365-023-01314-z
42. S.-Y. Xu, Z.-Q. Feng, Cluster emission in massive transfer reactions based on dinuclear system model. Nucl. Tech. (in Chinese) **46**, 030501 (2023). https://doi.org/10.11889/j.0253-3219.2023.hjs.46.030501
43. M.-H. Zhang, Y.-H. Zhang, J.-J. Li et al., Progress in transport models of heavy-ion collisions for the synthesis of superheavy nuclei. Nucl. Tech. (in Chinese) **46**, 080014 (2023). https://doi.org/10.11889/j.0253-3219.2023.hjs.46.080014
44. N. Wang, Z. Li, X. Wu, Improved quantum molecular dynamics model and its applications to fusion reaction near barrier. Phys. Rev. C **65**, 064608 (2002). https://doi.org/10.1103/PhysRevC.65.064608
45. X. Jiang, N. Wang, Probing the production mechanism of neutron-rich nuclei in multinucleon transfer reactions. Phys. Rev. C **101**, 014604 (2020). https://doi.org/10.1103/PhysRevC.101.014604
46. K. Zhao, Z. Liu, F.-S. Zhang et al., Production of neutron-rich $N = 126$ nuclei in multinucleon transfer reactions: omparison between ^{136}Xe $+^{198}$ Pt and ^{238}U $+^{198}$ Pt reactions. Phys. Lett. B **815**, 136101 (2021). https://doi.org/10.1016/j.physletb.2021.136101
47. C. Li, P.-W. Wen, J.-J. Li et al., Production mechanism of new neutron-rich heavy nuclei in the ^{136}Xe $+^{198}$ Pt reaction. Phys. Lett. B **776**, 278–283 (2018). https://doi.org/10.1016/j.physletb.2017.11.060
48. C. Li, J. Tian, F.-S. Zhang, Production mechanism of the neutron-rich nuclei in multinucleon transfer reactions: a reaction time scale analysis in energy dissipation process. Phys. Lett. B **809**, 135697 (2020). https://doi.org/10.1016/j.physletb.2020.135697
49. Y.-H. Zhang, J.-J. Li, C. Li et al., Microscopic study of the production of neutron-rich isotopes near $N = 126$ in the multinucleon transfer reactions ^{78,82,86}Kr $+^{208}$ Pb. Phys. Rev. C **109**, 044617 (2024). https://doi.org/10.1103/PhysRevC.109.044617
50. L. Li, F.-Y. Wang, Y.-X. Zhang, Isospin effects on intermediate mass fragments at intermediate energy-heavy ion collisions. Nucl. Sci. Tech. **33**, 58 (2022). https://doi.org/10.1007/s41365-022-01050-w
51. C. Golabek, C. Simenel, Collision dynamics of two ^{238}**U** atomic nuclei. Phys. Rev. Lett. **103**, 042701 (2009). https://doi.org/10.1103/PhysRevLett.103.042701
52. C. Simenel, Particle transfer reactions with the time-dependent Hartree-fock theory using a particle number projection technique. Phys. Rev. Lett. **105**, 192701 (2010). https://doi.org/10.1103/PhysRevLett.105.192701
53. C. Simenel, Particle-number fluctuations and correlations in transfer reactions obtained using the Balian-Vénéroni variational principle. Phys. Rev. Lett. **106**, 112502 (2011). https://doi.org/10.1103/PhysRevLett.106.112502
54. K. Sekizawa, TDHF theory and its extensions for the multinucleon transfer reaction: a mini review. Front. Phys **7**, 20 (2019). https://doi.org/10.3389/fphy.2019.00020
55. Z. Wu, L. Guo, Microscopic studies of production cross sections in multinucleon transfer reaction ^{58}Ni $+^{124}$ Sn. Phys. Rev. C **100**, 014612 (2019). https://doi.org/10.1103/PhysRevC.100.014612
56. J.-J. Li, N. Tang, Y.-H. Zhang et al., Progress on production cross-sections of unknown nuclei in fusion evaporation reactions and multinucleon transfer reactions. Int. J. Mod. Phys. E **32**, 2330002 (2023). https://doi.org/10.1142/S0218301323300023
57. Y.-Q. Xin, N.-N. Ma, J.-G. Deng et al., Properties of Z=114 superheavy nuclei. Nucl. Sci. Tech. **32**, 55 (2021). https://doi.org/10.1007/s41365-021-00899-7
58. F. Niu, P.-H. Chen, Z.-Q. Feng, Systematics on production of superheavy nuclei $Z = 119 - 122$ in fusion-evaporation reactions. Nucl. Sci. Tech. **32**, 103 (2021). https://doi.org/10.1007/s41365-021-00946-3
59. M.-H. Zhang, Y.-H. Zhang, Y. Zou et al., Predictions of synthesizing elements with $Z = 119$ and 120 in fusion reactions. Phys. Rev. C **109**, 014622 (2024). https://doi.org/10.1103/PhysRevC.109.014622
60. B. Li, N. Tang, Y.-H. Zhang et al., Production of p-rich nuclei with Z=20-25 based on radioactive ion beams. Nucl. Sci. Tech. **33**, 55 (2022). https://doi.org/10.1007/s41365-022-01048-4
61. L. Zhu, C. Li, C.-C. Guo et al., Theoretical progress on production of isotopes in the multinucleon transfer process. Int. J. Mod. Phys. E **29**, 2030004 (2020). https://doi.org/10.1142/S0218301320300040
62. Y. Zou, Y.-H. Zhang, N. Tang et al., Key problems to be solved possibly using machine learning in heavy ion collisions. Atom. Energy Sci. Tech. **57**, 762–773 (2023)
63. Z. Wang, Z.-Z. Ren, Predictions of the decay properties of the superheavy nuclei ^{293,294}119 and ^{294,295}120. Nucl. Tech. (in Chinese) **46**, 080011 (2023). https://doi.org/10.11889/j.0253-3219.2023.hjs.46.080011
64. Y. Chen, Y.-L. Ye, K. Wei, Progress and perspective of the research on exotic structures of unstable nuclei. Nucl. Tech. (in Chinese) **46**, 080020 (2023). https://doi.org/10.11889/j.0253-3219.2023.hjs.46.080020
65. S. Amano, Y. Aritomo, M. Ohta, Modes of massive nucleon transfer appearing in quasifission processes for collisions of superheavy nuclei. Phys. Rev. C **106**, 024610 (2022). https://doi.org/10.1103/PhysRevC.106.024610
66. S. Amano, Y. Aritomo, M. Ohta, Effects of neck and nuclear orientations on the mass drift in heavy ion collisions. Phys. Rev. C **109**, 034603 (2024). https://doi.org/10.1103/PhysRevC.109.034603
67. F.-C. Dai, P.-W. Wen, C.-J. Lin et al., Theoretical study of multinucleon transfer reactions by coupling the Langevin dynamics iteratively with the master equation. Phys. Rev. C **109**, 024617 (2024). https://doi.org/10.1103/PhysRevC.109.024617
68. L. Zhu, New model based on coupling the master and Langevin equations in the study of multinucleon transfer reactions. Phys. Lett. B **849**, 138423 (2024). https://doi.org/10.1016/j.physletb.2023.138423
69. J. Maruhn, W. Greiner, The asymmetrie two center shell model. Z. Physik **251**, 431–457 (1972). https://doi.org/10.1007/BF01391737

70. K.T.R. Davies, A.J. Sierk, J.R. Nix, Effect of viscosity on the dynamics of fission. Phys. Rev. C **13**, 2385–2403 (1976). https://doi.org/10.1103/PhysRevC.13.2385
71. P. Nadtochy, E. Ryabov, A. Karpov et al., Transport coefficients for modeling fission dynamics. Comput. Phys. Commun. **275**, 108308 (2022). https://doi.org/10.1016/j.cpc.2022.108308
72. A.J. Sierk, J.R. Nix, Fission in a wall-and-window one-body-dissipation model. Phys. Rev. C **21**, 982–987 (1980). https://doi.org/10.1103/PhysRevC.21.982
73. G. Adeev, A. Karpov, P. Nadtochii et al., Multidimensional stochastic approach to the fission dynamics of excited nuclei. Phys. Part. Nucl. **36**, 378–426 (2005)
74. J. Tian, W. Ye, Investigating nuclear dissipation properties at large deformations via excitation energy at scission. Nucl. Sci. Tech. **27**, 145 (2016). https://doi.org/10.1007/s41365-016-0146-y
75. H.J. Krappe, J.R. Nix, A.J. Sierk, Unified nuclear potential for heavy-ion elastic scattering, fusion, fission, and ground-state masses and deformations. Phys. Rev. C **20**, 992–1013 (1979). https://doi.org/10.1103/PhysRevC.20.992
76. A.J. Sierk, Macroscopic model of rotating nuclei. Phys. Rev. C **33**, 2039–2053 (1986). https://doi.org/10.1103/PhysRevC.33.2039
77. V. Zagrebaev, A. Karpov, Y. Aritomo et al., Potential energy of a heavy nuclear system in fusion-fission processes. Phys. Part. Nucl **38**, 469–491 (2007). https://doi.org/10.1134/S106377960704003X
78. P. Nadtochy, E. Ryabov, A. Karpov et al., Potential energy models of excited compound nucleus. Comput. Phys. Commun. **258**, 107605 (2021). https://doi.org/10.1016/j.cpc.2020.107605
79. S. Yamaji, H. Hofmann, R. Samhammer, Self-consistent transport coefficients for average collective motion at moderately high temperatures. Nucl. Phys. A **475**, 487–518 (1987). https://doi.org/10.1016/0375-9474(87)90075-3
80. L. Moretto, J. Sventek, A theoretical approach to the problem of partial equilibration in heavy ion reactions. Phys. Lett. B **58**, 26–30 (1975). https://doi.org/10.1016/0370-2693(75)90718-2
81. D.H.E. Gross, H. Kalinowski, Friction model of heavy-ion collisions. Phys. Rep. **45**(3), 175–210 (1978). https://doi.org/10.1016/0370-1573(78)90031-5
82. J. Galin, Experimental situation in deep inelastic reactions with respect to the rapidly relaxed modes. J. Phys. Colloques **37**, 83–107 (1976). https://doi.org/10.1051/jphyscol:1976506
83. W. Schröder, J. Birkelund, J. Huizenga et al., Mechanisms of very heavy-ion collisions: the ^{209}Bi $+^{136}$ Xe reaction at $E_{\mathrm{Lab}} = 1130$ MeV. Phys. Rep. **45**, 301–343 (1978). https://doi.org/10.1016/0370-1573(78)90110-2